Provided for non-commercial research and education use.
Not for reproduction, distribution or commercial use.

This article appeared in a journal published by Elsevier. The attached copy is furnished to the author for internal non-commercial research and education use, including for instruction at the authors institution and sharing with colleagues.

Other uses, including reproduction and distribution, or selling or licensing copies, or posting to personal, institutional or third party websites are prohibited.

In most cases authors are permitted to post their version of the article (e.g. in Word or Tex form) to their personal website or institutional repository. Authors requiring further information regarding Elsevier's archiving and manuscript policies are encouraged to visit:

http://www.elsevier.com/copyright

Author's personal copy

Journal of Electron Spectroscopy and Related Phenomena 184 (2011) 170–173

Contents lists available at ScienceDirect

Journal of Electron Spectroscopy and Related Phenomena

journal homepage: www.elsevier.com/locate/elspec

Recent advances in the determination of atomic parameters for modeling K lines in cosmically abundant elements

P. Quinet[a,b,*], P. Palmeri[a], C. Mendoza[c], M.A. Bautista[d], J. Garcia[e,f], M.C. Witthoeft[f], T.R. Kallman[f]

[a] Astrophysique et Spectroscopie, Université de Mons–UMONS, B-7000 Mons, Belgium
[b] IPNAS, Université de Liège, Sart Tilman, B-4000 Liège, Belgium
[c] Centro de Fisica, IVIC, Caracas 1020A, Venezuela
[d] Department of Physics, Western Michigan University, Kalamazoo, MI 49008, USA
[e] IACS-Department of Physics, The Catholic University of America, Washington, DC 20064, USA
[f] NASA Goddard Space Flight Center, Greenbelt, MD 20771, USA

ARTICLE INFO

Article history:
Available online 30 December 2010

Keywords:
Atomic processes
K-lines
Radiative rates
Auger rates
Photoionization

ABSTRACT

Over the last several years, our group has undertaken a systematic investigation of atomic properties of K-vacancy states in many ions. More precisely, reliable data such as level energies, wavelengths, Einstein *A*-coefficients, radiative and Auger widths were computed for a large number of ions using three different atomic structure theoretical approaches, i.e. relativistic Hartree–Fock (HFR), AUTOSTRUCTURE (AS) and multiconfiguration Dirac–Fock (MCDF) methods. Extensive calculations of photoabsorption and photoionization cross sections were also performed using the Breit–Pauli *R*-matrix method including the effects of radiative and Auger damping by means of an optical potential. Here, we report on our overall progress concerning N, O, Ne, Mg, Al, Si, S, Ar, Ca, Fe and Ni ions.

© 2010 Elsevier B.V. All rights reserved.

1. Introduction

The unprecedented spectral capabilities and sensitivity of recent orbiting X-ray telescopes (Chandra, XMM-Newton, Suzaku) have opened the door for quantitatively accurate studies of atomic inner-shell processes in astrophysical plasmas. In particular, the spectra from black holes and neutron stars contain inner-shell absorption lines from a large number of ions. This trend will continue to grow with the launch of future instruments such as the International X-ray Observatory (IXO). Such inner-shell processes, particularly K-shell processes, are observed in the spectral band of the observatories from all ionic stages (i.e. not just H-like or He-like) of the most abundant elements [1]. It is worth emphasizing that both fluorescent emission and Kα photoabsorption are observed in Chandra and XMM-Newton spectra, though never so far from the same source. These spectra are extremely valuable for they can be used to diagnose the conditions of the plasma and its chemical composition. Until recently, however, atomic parameters for modeling K lines were not available.

Over the last several years, our team has dedicated significant efforts toward the study of K-shell processes using different theoretical approaches. Here we present an overview of our recent progress in ions of the N, O, Ne, Mg, Al, Si, S, Ar, Ca, Fe and Ni isonuclear sequences for which complete data sets of level energies, wavelengths, radiative and Auger rates for K lines have been calculated. For most of these ions, K-shell photoionization cross sections were also computed.

2. Radiative and Auger rate calculations

Three independent methods were used in our work for atomic structure calculations. The main body of data was computed with the pseudo-relativistic Hartree–Fock (HFR) approach of Cowan [2]. Data accuracy was assessed by means of two other methods: the multiconfiguration Breit–Pauli method, which incorporates a scaled Thomas–Fermi–Dirac statistical potential as implemented in AUTOSTRUCTURE [3,4] and the General Relativistic Atomic Structure Package (GRASP) based on the multiconfiguration Dirac–Fock (MCDF) method [5,6].

In HFR and AUTOSTRUCTURE, wave functions are calculated with the Breit–Pauli relativistic corrections

$$H_{\mathrm{BP}} = H_{\mathrm{NR}} + H_{\mathrm{1B}} + H_{\mathrm{2B}} \tag{1}$$

where H_{NR} is the usual nonrelativistic Hamiltonian. The one-body relativistic operators

$$H_{\mathrm{1B}} = \sum_{n=1}^{N} f_n(\mathrm{SO}) + f_n(\mathrm{mass}) + f_n(\mathrm{D}) \tag{2}$$

* Corresponding author at: Astrophysique et Spectroscopie, Université de Mons–UMONS, B-7000 Mons, Belgium.
E-mail address: quinet@umons.ac.be (P. Quinet).

0368-2048/$ – see front matter © 2010 Elsevier B.V. All rights reserved.
doi:10.1016/j.elspec.2010.12.027

Author's personal copy

represent the spin-orbit interaction, f_n(SO), the non-fine-structure mass variation, f_n(mass), and the one-body Darwin correction, f_n(D). The two-body Breit operators are given by

$$H_{2B} = \sum_{n<m} g_{nm}(\mathrm{SO}) + g_{nm}(\mathrm{SS}) + g_{nm}(\mathrm{CSS}) + g_{nm}(\mathrm{D}) + g_{nm}(\mathrm{OO}) \quad (3)$$

where the g_{nm}(SO), g_{nm}(SS), g_{nm}(CSS), g_{nm}(D) and g_{nm}(OO) are the spin-other-orbit, the mutual spin–spin, the spin–spin contact, the two body Darwin and the orbit–orbit terms. HFR computes energies, Einstein A-coefficients and Auger rates with nonorthogonal orbital bases, which are generated by optimizing the average energy of each configuration. It also neglects the part of the two-body Breit operator (3). AUTOSTRUCTURE can use both orthogonal and nonorthogonal orbital bases for all the electronic configurations considered, which enables estimates of relaxation effects. Auger rates are computed in both HFR and AUTOSTRUCTURE in a distorted wave approach.

In the multiconfiguration Dirac–Fock method (MCDF), each atomic state function (ASF) is represented as a superposition of configuration state functions (CSF) of the type

$$\Psi(\alpha \Pi J M) = \sum_{i=1}^{n_c} c_i(\alpha) \Phi(\beta_i \Pi J M) \quad (4)$$

where Ψ and Φ are, respectively, the ASF and CSF; Π, J and M are the relevant quantum numbers for parity, total angular momentum and its associated total magnetic number; α and β_i stand for all the other quantum numbers that are necessary to describe unambiguously the ASFs and CSFs. The summation in Eq. (4) is up to n_c, the number of CSFs in the expansion, and each CSF is built from antisymetrized products of relativistic spin orbitals. The c_i coefficients, together with the orbitals, are optimized by minimizing an energy functional, the latter being built from one or more eigenvalues of the Dirac–Coulomb Hamiltonian depending on the optimization option adopted. In our work, we have used the extended average level (EAL) option in which the $(2J+1)$ weighted trace of the Hamiltonian is minimized. Transverse Breit interaction as well as other QED interactions, e.g. the vacuum polarization and self-energy, have been included in the Hamiltonian matrix as perturbations. Unfortunately, the GRASP code does not treat the continuum and has thus been exclusively employed in comparisons of radiative data for bound–bound transitions.

Up to now, in our recent studies, radiative and Auger decay data have been calculated for modeling the K lines of the nitrogen, oxygen, neon, magnesium, aluminium, silicium, sulfur, argon, calcium, iron and nickel isonuclear sequences. More precisely, level energies, transition wavelengths, radiative transition probabilities and radiative and Auger widths have been determined for all the ions along these sequences. The details of the theoretical procedures used can be found in the references listed in Table 1. Numerical results and detailed comparisons between the different methods considered in our work are also given in these original references. As examples, we show in Figs. 1 and 2 the comparisons between radiative and Auger decay rates obtained using the different approaches considered in our work for all nitrogen and aluminium ions, respectively. As illustrated in these figures, the general agreement between the different sets of data is very good, particularly for the strongest K-lines, i.e. those having radiative and Auger widths greater than 10^{12} s^{-1}, for which the average discrepancy does not exceed a few percent if we except a handful of K-vacancy levels in nitrogen ions for which larger discrepancies (mainly due to level admixture) are observed. As discussed in [14], these levels are $1s(^2S)2s2p^3(^5S^\circ)^4S_{3/2}^\circ$, $1s(^2S)2s2p^3(^3S^\circ)^2S_{1/2}^\circ$, $1s(^2S)2s2p^3(^1P^\circ)^2P_{1/2}^\circ$ (N III), $1s(^2S)2s2p^2(^4P)^3P_{0,1,2}$, $1s(^2S)2s2p^2(^2P)^1P_1$ (N IV) and $1s(^2S)2s2p(^3P^\circ)^2P_{1/2,3/2}^\circ$ (N V). We also note that the general agreement between our different theoretical approaches seems to improve when increasing the nuclear charge. This is essentially due to the fact that the interaction between $n=2$ and $n=3$ configuration complexes (considered in our HFR model only) are more important for the lowest ionization stages.

Table 1
Isonuclear sequences for which radiative and Auger decay rates for K-lines have been calculated in the present work.

Z	Isonuclear sequence	Ions	Refs.
7	Nitrogen	N I–N VI	[14]
8	Oxygen	O I–O VII	[15]
10	Neon	Ne I–Ne IX	[16]
12	Magnesium	Mg I–Mg XI	[16]
13	Aluminium	Al I–Al XII	[17]
14	Silicium	Si I–Si XIII	[16]
16	Sulfur	S I–S XV	[16]
18	Argon	Ar I–Ar XVII	[16]
20	Calcium	Ca I–Ca XIX	[16]
	Iron	Fe II–Fe IX	[18]
26		Fe X–Fe XVII	[19]
		Fe XVIII–Fe XXV	[20]
28	Nickel	Ni II–Ni XXVII	[21]

3. K-shell photoionization and photoabsorption cross sections

Resonances have a large contribution to the photoabsorption cross-section near the K edge. The Auger rates for levels with a K-vacancy tend to be large leading to an ejected electron even if the incident photon does not have enough energy to directly ionize the K-electron. There are two basic types of Auger processes, participa-

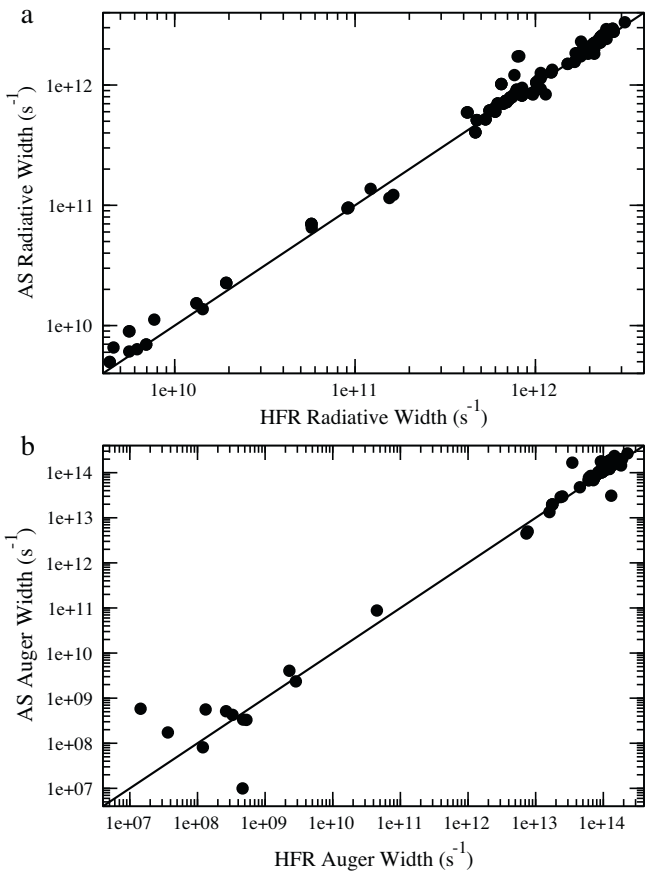

Fig. 1. Comparison between HFR and AUTOSTRUCTURE (AS) calculations for radiative (a) and Auger (b) widths in nitrogen ions.

Author's personal copy

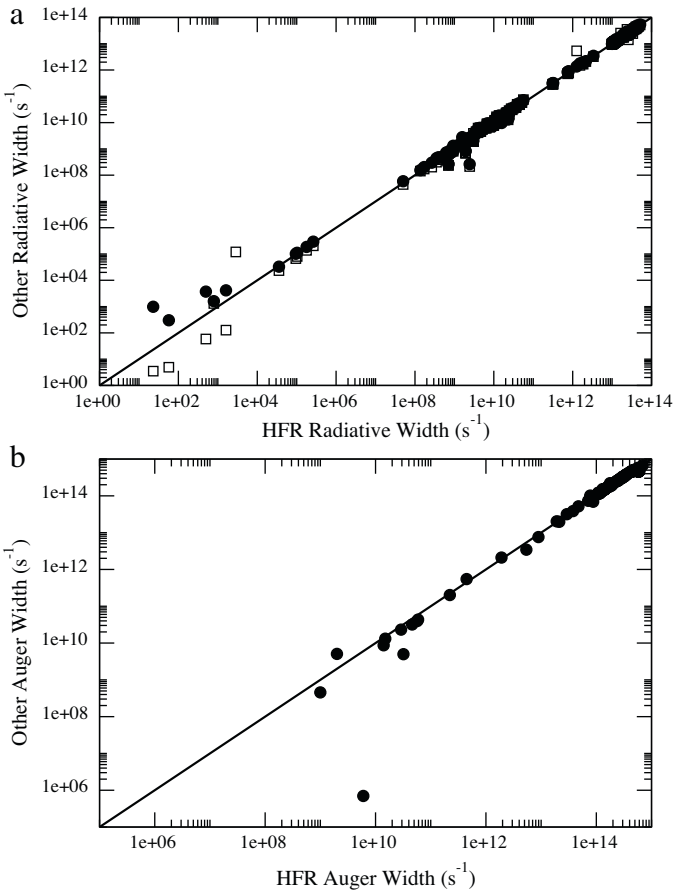

Fig. 2. Comparison of HFR radiative (a) and Auger (b) widths with AUTOSTRUCTURE (full circles) and MCDF (open squares) values for aluminium ions.

tor and spectator. In the participator process, the excited electron is involved in the Auger process while, in the spectator decay, it is core relaxation which yields the Auger electron. A further complication comes from the fact that the excited state can radiatively stabilize instead of undergoing the Auger process meaning no photoionization occurs. All of these processes are shown in Fig. 3 and must be included in the calculations.

In our work, photoionization and photoabsorption cross sections were computed with the Breit–Pauli *R*-Matrix code [7,8]. In this approach, wave functions for states of an *N*-electron target and a colliding electron with total angular momentum and parity $J\,\Pi$ are expanded in terms of the target eigenfunctions

$$\Psi^{J\Pi} = A\sum_i \chi \frac{F_i(r)}{r} + \sum_j c_j \Phi_j \qquad (5)$$

where the χ_i functions are vector coupled products of the target eigenfunctions and the angular components of the incident-electron functions; $F_i(r)$ are the radial part of the continuum wave functions that describe the motion of the scattered electron and A is an antisymetrization operator. The functions Φ_j are bound-type functions of the total system constructed with target orbitals. The Breit–Pauli relativistic version has been developed in [9,10] and Auger and radiative dampings were taken into account by means of an optical potential [11–13] where the resonance energy with respect to the threshold acquires an imaginary component.

Since an *R*-matrix calculation involves several steps and there are dozens of ions to calculate, we have developed a script which can run through the entire calculation using a single input file. This saves a lot of hands-on time and provides consistency to our calculations. The script also contains a method to automatically resolve the resonance structure ensuring a converged cross-section.

For ions with 10 or fewer electrons, our target expansion was $1s^2 l^n$ and $1s l^{n+1}$ where $n+2$ is the total number of electrons. Systems with more than 10 electrons included configurations of the type $1s^2 2l^6 3l^n$, $1s^2 2l^6 3l^{n-1}3d$, $1s^2 2l^5 3l^{n+1}$ and $1s2l^6 3l^{n+1}$ (l = s, p) where $n+8$ is the total number of electrons. Also the 2s- and 2p-hole levels were included for these systems in addition to the 1s-hole levels. For neutral systems, a larger target expansion was needed due to configuration mixing. The expansion for these atoms was determined individually. The radial wave functions used in our cross section calculations were those obtained from AUTOSTRUCTURE, but the energies were adjusted using the HFR code.

In Table 2, we present a list of ions for which K-shell photoionization cross sections have been computed so far. In each paper mentioned in this table, the calculations are described in details and comparisons are made with previous data when available. The full cross sections can be found in these original publications as on-line tables.

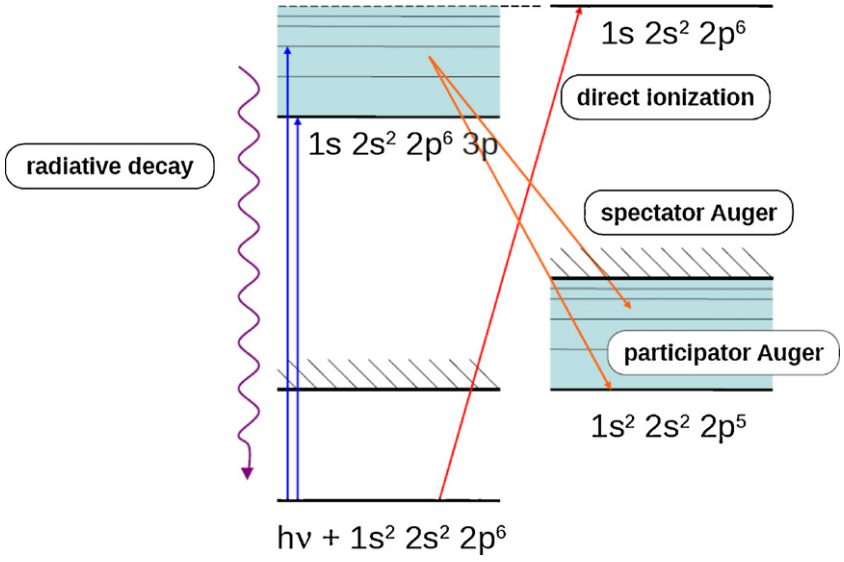

Fig. 3. An example of the different processes to be included in K-shell photoionization calculations.

Author's personal copy

Table 2
K-shell photoionization cross sections computed in the present work up to now. BP indicates that the calculations are level-resolved using the Breit–Pauli *R*-matrix codes, while LS means that the calculations are only term-resolved. The number between brackets indicates the reference for the data.

	N	O	Ne	Mg	Si	S	Ar	Ca	Fe	Ni
Li-like	BP [14]	BP [15]	BP [22]	BP [22]	BP [22]	BP [22]	BP [22]	BP [22]	BP [23]	BP [25]
Be-like	BP [14]	BP [15]	BP [22]	BP [22]	BP [22]	BP [22]	BP [22]	BP [22]	BP [24]	BP [25]
B-like	BP [14]	BP [15]	BP [22]	BP [22]	BP [22]	BP [22]	BP [22]	BP [22]	BP [24]	BP [25]
C-like	BP [14]	BP [15]	BP [22]	BP [22]	BP [22]	BP [22]	BP [22]	BP [22]	BP [24]	BP [25]
N-like	LS [14]	LS [15]	BP [22]	BP [22]	BP [22]	BP [22]	BP [22]	BP [22]	BP [24]	BP [25]
O-like		LS [15]	BP [22]	BP [22]	BP [22]	BP [22]	BP [22]	BP [22]	BP [24]	BP [25]
F-like			BP [22]	BP [22]	BP [22]	BP [22]	BP [22]	BP [22]	BP[24]	BP [25]
Ne-like			LS [22]	BP [22]	BP[22]	BP [22]	BP [22]	BP[22]	BP [24]	BP[25]
Na-like				BP [26]	BP [26]	BP [26]	BP [26]	BP [26]	BP [27]	BP [25]
Mg-like					BP [26]	BP [26]	BP [26]	BP [26]	LS [27]	LS [25]
Al-like					LS [26]	LS [26]	LS [26]	LS [26]	LS [27]	LS [25]
Si-like						LS [26]	LS [26]	LS [26]	LS [27]	LS [25]
P-like						LS [26]	LS [26]	LS [26]	LS [27]	LS [25]
S-like							LS [26]	LS [26]	LS [27]	LS [25]
Cl-like							LS [26]	LS [26]	LS [27]	LS [25]
Ar-like								LS [26]	LS [27]	LS [25]
K-like								LS [26]		LS [25]
Ca-like										LS [25]

4. Conclusion

In the present paper, we have presented an overview of our recent calculations concerning the atomic parameters associated with K-vacancy states in cosmically abundant ions such as those belonging to the N, O, Ne, Mg, Al, Si, S, Ar, Ca, Fe and Ni isonuclear sequences. These new data will be incorporated in the XSTAR modeling code [27] in order to generate improved opacities in the K-edge regions of the elements considered, which will lead to useful astrophysical diagnostics when all collisional calculations (in progress) will be finished.

Nevertheless, the different works summarized here have already allowed us to highlight some interesting results. Amongst them, let us mention that, in the study of decay properties of K-vacancy states in Fe X–Fe XVII ions [19], the Kα radiative and KLL Auger widths have been found to be nearly independent of both the outer-electron configuration and outer-subshell occupancies. This has important consequences on the opacities close to the K edge as demonstrated in iron [28].

Acknowledgments

This work was funded in part by the NASA Astronomy and Physics Research and Analysis Program. The Belgian F.R.S.-FNRS is also acknowledged for financial support. PP and PQ are respectively Senior Research Associate and Research Associate of this organization.

References

[1] F.B.S. Paerels, S.M. Kahn, Ann. Rev. Astron. Astrophys. 41 (2003) 291.
[2] R.D. Cowan, The Theory of Atomic Structure and Spectra, University of California Press, Berkeley, 1981.
[3] N.R. Badnell, J. Phys. B: At. Mol. Opt. Phys. 19 (1986) 3827.
[4] N.R. Badnell, J. Phys. B: At. Mol. Opt. Phys. 30 (1997) 1.
[5] I.P. Grant, B.J. McKenzie, P.H. Norrington, D.F. Mayers, N.C. Pyper, Comput. Phys. Commun. 21 (1980) 207.
[6] B.J. McKenzie, I.P. Grant, P.H. Norrington, Comput. Phys. Commun. 21 (1980) 233.
[7] M.J. Seaton, J. Phys. B: At. Mol. Opt. Phys. 20 (1987) 6363.
[8] K.A. Berrington, P.G. Burke, K. Butler, M.J. Seaton, P.J. Storey, K.T. Taylor, Y. Yan, J. Phys. B: At. Mol. Opt. Phys. 20 (1987) 6379.
[9] N.S. Scott, P.G. Burke, J. Phys. B: At. Mol. Opt. Phys. 13 (1980) 4299.
[10] N.S. Scott, K.T. Taylor, Comput. Phys. Commun. 25 (1982) 347.
[11] F. Robicheaux, T.W. Gorczyca, M.S. Pindzola, N.R. Badnell, Phys. Rev. A 52 (1995) 1319.
[12] T.W. Gorczyca, N.R. Badnell, J. Phys. B: At. Mol. Opt. Phys. 29 (1996) L283.
[13] T.W. Gorczyca, B.M. McLaughlin, J. Phys. B: At. Mol. Opt. Phys. 33 (2000) L859.
[14] J. Garcia, T.R. Kallman, M. Witthoeft, E. Behar, C. Mendoza, P. Palmeri, P. Quinet, M.A. Bautista, M. Klapisch, Astrophys. J. Suppl. 185 (2009) 477.
[15] J. Garcia, C. Mendoza, M.A. Bautista, T.W. Gorczyca, T.R. Kallman, P. Palmeri, Astrophys. J. Suppl. 158 (2005) 68.
[16] P. Palmeri, P. Quinet, C. Mendoza, M.A. Bautista, J. Garcia, T.R. Kallman, Astrophys. J. Suppl. 177 (2008) 408.
[17] P. Palmeri, P. Quinet, C. Mendoza, M.A. Bautista, J. Garcia, M.C. Witthoeft, T.R. Kallman, Astron. Astrophys. 525 (2011) A59.
[18] P. Palmeri, C. Mendoza, T.R. Kallman, M.A. Bautista, M. Meléndez, Astron. Astrophys. 410 (2003) 359.
[19] C. Mendoza, T.R. Kallman, M.A. Bautista, P. Palmeri, Astron. Astrophys. 414 (2004) 377.
[20] P. Palmeri, C. Mendoza, T.R. Kallman, M.A. Bautista, Astron. Astrophys. 403 (2003) 1175.
[21] P. Palmeri, P. Quinet, C. Mendoza, M.A. Bautista, J. Garcia, M.C. Witthoeft, T.R. Kallman, Astrophys. J. Suppl. 179 (2008) 542.
[22] M.C. Witthoeft, M.A. Bautista, C. Mendoza, T.R. Kallman, P. Palmeri, P. Quinet, Astrophys. J. Suppl. 182 (2009) 127.
[23] M.A. Bautista, C. Mendoza, T.R. Kallman, P. Palmeri, Astron. Astrophys. 403 (2003) 339.
[24] M.A. Bautista, C. Mendoza, T.R. Kallman, P. Palmeri, Astron. Astrophys. 418 (2004) 1171.
[25] M.C. Witthoeft et al., in preparation.
[26] M.C. Witthoeft, J. Garcia, T.R. Kallman, M.A. Bautista, C. Mendoza, P. Palmeri, P. Quinet, Astrophys. J. Suppl. 192 (2011) 7.
[27] T.R. Kallman, M.A. Bautista, Astrophys. J. Suppl. 133 (2001) 221.
[28] P. Palmeri, C. Mendoza, T.R. Kallman, M.A. Bautista, Astrophys. J. 577 (2002) L119.